A NEW MULTIFIELD FINITE ELEMENT METHOD IN STEADY STATE HEAT ANALYSIS

by

Dubravka M. MIJUCA, Ana M. ŽIBERNA, and Bojan I. MEDJO

A new original primal-mixed finite element approach and related hexahedral finite element HC:T/q for the analysis of behavior of solid bodies under thermal loading is presented. The essential contributions of the present approach is the treatment of temperature and heat flux as fundamental variables that are simultaneously calculated, as well as capability to introduce initial and prescribed temperature and heat flux. In order to minimize accuracy error and enable introductions of flux constraints, the tensorial character of the present finite element equations is fully respected. The proposed finite element is subjected to some standard benchmark tests in order to test convergence of the results, which enlighten the effectiveness and reliability of the approach proposed.

Key words: *steady state heat, finite elements, mixed formulation*

Introduction

Increased thermal efficiency and the integrity of materials in high-temperature environments is an essential requirement in modem engineering structures in, automotive, aerospace, nuclear, offshore, environmental and other industries. Nowadays, the finite element method is used regularly to obtain numerical solutions for heat transfer problems. The most common choice when using finite elements is standard Galerkin formulation [1, 2].

In the present paper a new original finite element approach for solving steady state heat transfer in the solid body, is presented. The main motive for the present investigation is found in the lack of hexahedral (solid) finite element that is reliable [1] and robust, mainly in accordance to change of its aspect ratio. In addition, the motive is also found in the need for the finite element procedure which treats both variables of interest, temperature and heat flux, as fundamental ones [2]. Moreover, the motive is found in well-known problem of connecting finite elements of different dimensionality, i.e. when a model problem has geometrical transitions from solid to thick or thin shell/plate.

Further, the main objective of the present investigation is to show that a new reliable [1] mixed hexahedral (brick) finite element HC:*T/q* [2] can be used in the analysis of engineering constructions of arbitrary shape, so without need for *a posteriori* calculation of heat fluxes. Thus, on the contrary to the primal approach, present finite element ap-

proach has two fundamental variables, temperature and heat flux, which are calculated simultaneously.

Consequently, the main goal of the present investigation is to validate the use of the new finite element HC:T/q in steady state heat analysis of isotropic, orthotropic or multi-material solid bodies under different thermal or mechanical loading scenarios.

The future investigation is oriented toward implementation of the present approach in the existing in-house primal-mixed elasticity code [5] for more accurate determination of thermal stresses, where no consistency problem will occur in calculation of thermal and mechanical deformations [3, 4].

Weak form of the steady state heat field equations

Let us consider a body which occupies some closed and bounded domain $\overline{\Omega}$ of the Euclidian space E^n ($n = 1, 2, 3$). The inner part of $\overline{\Omega}$ is denoted by Ω, and its boundary by $\partial \Omega, \Omega \quad \partial \Omega \quad \overline{\Omega}$. The boundary is subdivided into four parts: $\partial \Omega_T, \partial \Omega_q, \partial \Omega_c$, and $\partial \Omega_r$ which are: part of the boundary per temperature, heat flux, heat flux due to the convection, and heat flux due to the radiation, respectively, such that $\partial \Omega_T \cup \partial \Omega_q \cup \partial \Omega_c \cup \partial \Omega_r \subset \partial \Omega$. The state of the body is described by temperature T and heat flux vector $\boldsymbol{q}$. Let us consider a complete system of field equations for steady-state heat transfer in the strong form, where:

$$\text{div}\boldsymbol{q} + f = 0 \ \text{in} \ \Omega \tag{1}$$

$$\boldsymbol{q} = -\boldsymbol{k}\nabla T \ \text{in} \ \Omega \tag{2}$$

are respectively, the equation of thermal balance that states that the divergence of the heat flux is equal to the internal heat source f, and Fourier's law of heat conduction, which assumes that the heat flux is linearly related to the negative gradient of the temperature, where $\boldsymbol{k}$ is second order tensor of thermal conductivity, which is heat transfer property of an general orthotropic material. If the material is homogeneous and isotropic, the tensor $\boldsymbol{k}$ will degenerate to simple scalar value k, *i. e.* thermal conductivity coefficient. Nevertheless, the present approach considers full tensor of thermal conductivity.

These two equations are subjected to the following boundary conditions:

$$T \quad \overline{T} \ \text{on} \ \partial \Omega_T \tag{3}$$

$$\boldsymbol{q} = \boldsymbol{q}_h = h \ \text{on} \ \partial \Omega_q \tag{4}$$

$$\boldsymbol{q} = q_c = h_c(T - T_a) \ \text{on} \ \partial \Omega_c \tag{5}$$

$$\boldsymbol{q} \quad q_r \quad h_r \sigma A(T^4 \quad T_a^4) \ \text{on} \ \partial \Omega_r \tag{6}$$

which are, boundary conditions per temperature (3) and per heat flux (4)-(6). More clearly, boundary conditions due to the prescribed heat flux are given by the expression

(4). Further, boundary conditions due to the convection are given by the expression (5), where h_c is the convective coefficient and T_a is the temperature of the surrounding medium. Finally, boundary conditions due to the radiation (6) are not presently considered.

Let us suppose that boundary condition (3) is essential, and hence exactly satisfied by the trial functions of a problem. Then we need to consider only the weak forms of the eqs. (1) and (2). Using the Galerkin procedure, one can seek the weak solution of eq. (1):

$$\int_{\Omega} (\mathrm{div}\, \boldsymbol{q} - f)\theta \, \mathrm{d}\Omega = 0 \qquad (7)$$

where θ denotes test functions in the complete space of the interpolation function, which are taken from the Hilbert space L_2 of all real measurable square integral scalar functions: $\int_{\Omega} g^2 \mathrm{d}\Omega < \infty$, with the inner product $(h,g) = \int_{\Omega} hg \mathrm{d}\Omega$ and the norm defined by $\|g\|^2 = (g,g)$ for all $h, g \in L_2(\Omega)$.

Further, we will consider the weak form of inverted constitutive eq. (2), where vector $\boldsymbol{Q}$ is the test function taken from the space of all measurable square integrable vector fields:

$$\int_{\Omega} (\boldsymbol{k}^{-1}\boldsymbol{q} - \nabla T)\boldsymbol{Q} \mathrm{d}\Omega = 0 \qquad (8)$$

Weak formulation of the mixed problem

Simple summation of eqs. (7) and (8) gives us the expression which represents asymmetric weak formulation of the mixed problem.

Find $\{T, \boldsymbol{q}\} \in H^1(\Omega) \times H(\mathrm{div})$ satisfying boundary conditions and

for all

$$\int_{\Omega} (\boldsymbol{k}^{-1}\boldsymbol{q} - \nabla T)\boldsymbol{Q} \mathrm{d}\Omega + \int_{\Omega} (\mathrm{div}\, \boldsymbol{q} - f)\theta \, \mathrm{d}\Omega$$

$$\{\theta, \boldsymbol{Q}\} \in L_2(\Omega) \times L_2(\Omega) \qquad (9)$$

In these expressions, $H(\mathrm{div})$ is the space of all vector fields which are square integrable and have square integrable divergence with the norm defined by $\|g\|^2 = \int_{\Omega} [(\mathrm{div}\, g)^2 + g^2] \mathrm{d}\Omega$ for all $g \in H(\mathrm{div})$.

However, it is a common opinion that asymmetric formulations are impractical from the computational point of view. Integrating by parts and applying divergence theorem on the first term on the right side of eq. (9) yields symmetric weak form of a mixed problem, where H^1 is the space of all scalar fields which are square integrable and have square integrable gradients, with the norm $\|g\|^2 = \int_{\Omega} [(\nabla g)^2 + g^2] \mathrm{d}\Omega$ for all $g \in H^1(\Omega)$:

Find $\{T, \boldsymbol{q}\} \in H^1(\Omega) \times L_2(\Omega)$ such that $T\big|_{\partial\Omega_T} = \overline{T}$ and

$$\int_\Omega \boldsymbol{qk}^{-1}\boldsymbol{Q}\mathrm{d}\Omega - \int_\Omega T\,\nabla\boldsymbol{Q}\mathrm{d}\Omega - \int_\Omega \nabla\boldsymbol{q}\,\theta\mathrm{d}\Omega - \int_\Omega \theta f\mathrm{d}\Omega - \int_{\partial\Omega_q}\theta q_h\mathrm{d}\partial\Omega - \int_{\partial\Omega_c}q_c\theta\mathrm{d}\partial\Omega \qquad (10)$$

for all $\{\theta, \boldsymbol{Q}\} \in H^1(\Omega){\times}L_2(\Omega)$ such that $\theta\big|_{\partial\Omega_T}\;\;0.$

Finite element approximation of the field equations

Let C_h be the partitioning of the domain Ω into elements Ω_i and let us define finite element subspaces for the temperature scalar T, the heat flux vector $\boldsymbol{q}$ and the appropriate test (weight) functions, respectively as:

$$T_h \quad \{T \quad H^1(\Omega){:}T\big|_{\partial\Omega_T} \quad \overline{T}, \quad T \quad T^L P_L(\Omega_i), \quad \Omega_i \quad C_h\}$$

$$\Theta_h \quad \{\theta \quad H^1(\Omega){:}\theta\big|_{\partial\Omega_T} \quad 0, \quad \theta \quad \theta^M P_M(\Omega), \quad \Omega_i \quad C_h\}$$

$$Q_h \quad \{\boldsymbol{q} \quad H^1(\Omega){:}\boldsymbol{q}\,\boldsymbol{n}\big|_{\partial\Omega_q} \quad h, \quad \boldsymbol{q}\,\boldsymbol{n}\big|_{\partial\Omega_c} \quad h_c(T \quad T_0), \quad \boldsymbol{q} \quad \boldsymbol{q}^L V_L(\Omega_i), \quad \Omega_i \quad C_h\}$$

$$\vartheta_h \quad \{\boldsymbol{Q} \quad H^1(\Omega){:}\boldsymbol{Q}\,\boldsymbol{n}\big|_{\partial\Omega_\theta\;\partial\Omega_c} \quad 0, \quad \boldsymbol{Q} \quad \boldsymbol{Q}^M V_M(\Omega_t), \quad \Omega_i \quad C_h\} \qquad (11)$$

In these expressions T^L and $\boldsymbol{q}^L$ are nodal values of the temperature scalar T and flux vector $\boldsymbol{q}$, respectively. Accordingly, P_L and V_L are corresponding values of the interpolation (local base) functions connecting temperatures and fluxes at an arbitrary point in Ω_i (the body of an element), and the nodal values of these quantities. The complete analogy holds for the temperature and flux weight functions θ and $\boldsymbol{Q}$. Please note that, as an essentially new approach, trial and test base functions for approximation of fluxes are presently chosen from the smaller, but continuous space H^1, that will provide the continuous heat flux picture over the domain of the model problem.

It should be noted that if present finite element approach is applied on model problems with abrupt material changes (multimaterials), where local heat flux discontinuity exists, the present rule (that local flux approximation functions are from continuous function space H^1) is too hard. It is left for future investigation to relax stress continuity on the interface surface(s) only, where fluxes will be chosen from space L^2 as in eq. (10). Nevertheless, it will be shown that this local violation does not affect expected target results in the vicinity or on the material interface.

Numerical implementation

By analogy with finite element approach in elasticity [5], after discretization of the starting problem using finite element method, present scheme can be written as a system of linear equations of order $n = n_q + n_T$, where n_T is the number of temperature degrees of freedom, while n_q is the number of flux degrees of freedom, in matrix form:

$$A_{vv} \quad B_{vv}^T \quad \boldsymbol{q}_v \quad A_{vp} \quad B_{vp}^T \quad \boldsymbol{q}_p \quad\quad 0$$
$$B_{vv} \quad D_{vv} \quad T_v \quad B_{vp} \quad D_{vp} \quad T_p \quad F_p \quad H_p \quad K_p \qquad (12)$$

114

In this expression, unknown (variable) and known (initial, prescribed) values of the fluxes and temperatures, denoted by the indices v and p respectively, are decomposed.

The nodal flux (q^{pL}) and temperature (T^L) components are consecutively ordered in the column matrices q and T respectively. The homogeneous and nonhomogenous essential boundary conditions per temperatures T_p and fluxes q_p are introduced as contribution to the right-hand side of the expression (12).

The members of the entry matrices A, B, and D, and the column matrices F, H, and K in expression (12), are respectively:

$$A_{LpMr} \quad \sum_e \int_{\Omega_e} g^a_{(L)p} V_L k_{ab}^{1} g^b_{(M)r} V_M \, \mathrm{d}\Omega_e; \quad B_{LpM} \quad \sum_e \int_{\Omega_e} g^a_{(L)p} V_L P_{M,a} \, \mathrm{d}\Omega_e$$

$$D_{LM} \quad \sum_e \int_{\partial\Omega_{ce}} h_c P_L P_M \, \partial\Omega_{ce}; \quad F_M \quad \sum_e \int_{\Omega_e} P_M f \mathrm{d}\Omega_e \qquad (13)$$

$$H_M \quad \sum_e \int_{\partial\Omega_{he}} P_M h \mathrm{d}\partial\Omega_{he}; \quad K_M \quad \sum_e \int_{\partial\Omega_{ce}} P_M h_c T_0 \mathrm{d}\partial\Omega_{ce}$$

In the above expressions, the Euclidian shifting operator $g^a_{(L)p}$ is given by $g^a_{(L)p}$ $\delta_{ij} g^{ac} (\partial z^i / \partial \xi^c)(\partial z^j / \partial y^{(L)p})$ where, $z^i (i, j, k, l = 1, 2, 3)$ is global Cartesian coordinate system of reference. Further, $y^{(L)r}(r, s, t = 1, 2, 3)$ is coordinate system at each global node L, per heat flux. Further, local natural (convective) coordinate systems per finite elements are denoted by $\xi^a(a, b, c, d = 1, 2, 3)$, while, g^{ab} and $g^{(L)mn}$ are components of the contravariant fundamental metric tensors, the first one with respect to natural coordinate system of a finite element ξ^a, and the second to $y^{(L)n}$ at global node L. Furthermore, $P_{M,a} \equiv \partial P_M / \partial \xi^a$. Since tensorial character is fully respected, one can easily choose appropriate coordinate system at each global node, useful for prescribing of fluxes and/or temperatures, or results interpretation.

It should be noted that matrix form expression (12) represents a new original form of resulting system of linear equations in the steady state heat analysis. Especially, because contribution from convective heat transfer represented by matrix entry is naturally assembled to specified position in expression (12) connected to temperature degrees of freedom.

Finite element HC8/27

Mixed finite element per temperature and flux, HC8/(9-27), is shown in fig. 1. Its acronym is taken from [5], where the first letter H stands for hexahedral element geometrical shape, while the letter C indicates the use of continuous approximation functions.

Temperature and heat flux fields are approximated at least by eight tri-linear shape functions connected to eight corner nodes (elements HC8/9, HC8/21, and HC8/27), or at least by twenty tri-quadratic shape functions connected to eight corner nodes and twelve mid-side nodes (elements HC20/21 and HC20/27). In addition, stabilization of finite element is achieved by full or partial hierarchic interpolation of heat flux. In case of the element HC8/(9-27) shape functions for flux are one order higher than for
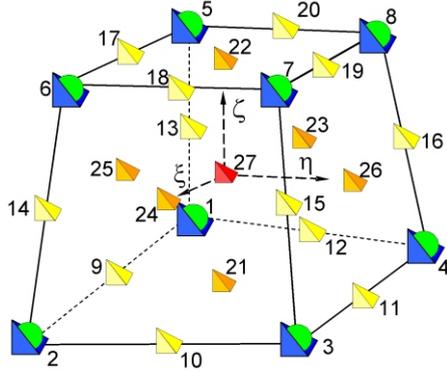
Figure 1. Finite element HC8/(9-27)

temperature, while for HC20/(21-27) they are both quadratic. Thus, for element HC20/27 twenty-seven flux nodes are available to accommodate full triquadratic expansion in natural coordinates ξ^a (a = 1, 2, 3). Consequently, following multifield combinations of temperature and flux nodes are available to user: HC8/9, HC8/21, HC8/27, HC20/21, and HC20/27. Moreover, per each corner node there is maximum four degrees of freedom n = 4 (one temperature degree of freedom n_T = 1 and three degrees of freedom per heat flux n_q = 3). For element HC20/(21-27) twelve mid-side nodes can also have degrees of freedom for flux and temperature. At hierarchical nodes there are only degrees of freedom connected to heat flux.

Solution of the resulting system of linear equations

In the present paper, the method based on multifrontal approach, one of the main categories of direct methods for solving of the resulting system of linear equations, is used. The core of that method is taken from the code MA47 [6], representing a version of sparse Gaussian elimination which is implemented using multifrontal method.

Low order tests

In order to check necessary and sufficient conditions for convergence, low order tests are traditionally the first steps in the validation process of each new finite element. In addition, some authors considered these tests as tools for assessment of robustness of finite element algorithms. In the present paper, necessary [10] and sufficient conditions [11, 12] solvability tests are considered.

Necessary conditions for solvability

It is considered that single finite element passes solvability test if number of its flux degrees of freedom n_q is greater than number of temperature degrees of freedom n_T. This test is known [10] as single element patch test. In case of the finite element HC8/27 we have n_T = 8 and n_q = 81. So evidently, it passes the present test. In addition, its simpler configurations, HC8/8 and HC8/9, pass the present test also, because $n_q^{\mathrm{HC8/8}}$ 24 and

$n_q^{\text{HC8/9}}$ 27, that are again greater than number of the temperature degrees of freedom $n_T = 8$.

Further, finite element HC20/20, HC20/21 and HC20/27, have $n_q^{\text{HC20/20}}$ 60, $n_q^{\text{HC20/21}}$ 63, and $n_q^{\text{HC20/27}}$ 81 flux degrees of freedom, respectively. So, for these finite elements, the number of heat flux degrees of freedom is evidently greater than the number of the temperature degrees of freedom $n_T = 20$. Consequently, for those elements necessary conditions for solvability are satisfied also.

Sufficient conditions for solvability
Eigenvalue analysis

In order to check if one finite element is sensitive to the locking phenomena, that is, to illustrate that element is free of spurious zero-energy modes (mechanisms), an eigenvalue analysis of single finite element is usually performed [12]. This test is also known as sufficient conditions for solvability test. It should be noted that presently one finite element free of boundary conditions, passes sufficient solvability test if number of zero eigenvalues of the relevant system matrix in eq. (12) is equal to one, from the reason that primal variable is scalar function.

For example, for finite element HC8/27, number of negative eigenvalues corresponds to number of temperature degrees of freedom $n_T = 8 \times 1 = 8$, while number of positive eigenvalues corresponds to number of flux degrees of freedom $n_q = 27 \times 3 = 81$.

In tabs. 1 and 2, calculated eigenvalues are sorted in increasing order. All eigenvalues connected to the temperature degrees of freedom are reported. On the other

Table 1. Eigenvalues for different one finite element configurations HC8/8, HC8/9, and HC8/27

Mode (dof)		HC8/8	HC8/9	HC8/27
1		−1.951941E−01	−2.290541E−01	−3.303563E−01
2		−1.951941E−01	−2.290541E−01	−3.303563E−01
3		−1.951941E−01	−2.290541E−01	−3.303563E−01
4	Temp	−9.884506E−02	−9.884506E−02	−1.560596E−01
5		−9.884506E−02	−9.884506E−02	−1.560596E−01
6		−9.884506E−02	−9.884506E−02	−1.560596E−01
7		−4.166667E−02	−4.166667E−02	−5.384102E−02
8	Zero	0	0	0
9		4.629630E−03	4.629630E−03	9.093757E−05
10-31				
32		3.201941E−01		
33-35	Flux			
36			4.685373E−01	
37-89				
90				1.290335E+00

117

hand, only the smallest and largest eigenvalue connected to flux degrees of freedom are reported here. We may also see that finite elements HC8/8, HC8/9 pass the present test, with number of negative eigenvalues equal to number of temperature degrees of freedom and positive eigenvalues equal to number of flux degrees of freedom, *i. e.* $n_q^{HC8/8}$ 24 and $n_q^{HC8/9}$ 27.

Results of the present test for finite elements, HC20/20, HC20/21, and HC20/27 are analogous, *i. e.* all of them pass the test, where number of negative eigenvalues is equal to 20, and the number of positive eigenvalues is equal to 60, 63, and 81, respectively.

Table 2. Eigenvalues for different one finite element configurations HC20/20, HC20/21, and HC20/27

ModE (dof)		HC20/20	HC20/21	HC20/27
1		−5.274123E-01	−5.628892E-01	−6.405245E-01
2		−5.274123E-01	−5.628892E-01	−6.405245E-01
3		−5.274123E-01	−5.628892E-01	−6.405245E-01
4		−4.693950E-01	−4.693950E-01	−5.465386E-01
5		−2.822907E-01	−2.822907E-01	−3.245214E-01
6		−2.822907E-01	−2.822907E-01	−3.245214E-01
7		−1.391434E-01	−1.391434E-01	−1.583908E-01
8		−1.391434E-01	−1.391434E-01	−1.583908E-01
9		−1.391434E-01	−1.391434E-01	−1.583908E-01
10	Temp	−8.229060E-02	−8.229060E-02	−8.810544E-02
11		−8.229060E-02	−8.229060E-02	−8.810544E-02
12		−8.229060E-02	−8.229060E-02	−8.810544E-02
13		−4.450799E-02	−4.649999E-02	−4.732059E-02
14		−4.450799E-02	−4.649999E-02	−4.732059E-02
15		−4.450799E-02	−4.649999E-02	−4.732059E-02
16		−4.117091E-02	−4.117092E-02	−4.117092E-02
17		−2.614909E-02	−2.614909E-02	−2.639023E-02
18		−2.614909E-02	−2.614909E-02	−2.639023E-02
19		−2.614909E-02	−2.614909E-02	−2.639023E-02
20	Zero	0	0	0
21		2.232664E-03	2.061110E-03	1.408515E-04
22-79				
80		3.718892E-01		
81-83	Flux			
84			1.191550E+00	
85-100				
101				1.645062E+00

High-order tests
The mathematical convergence requirements

As the finite element mesh is refined, solution of discrete problem should approach to the analytical solution of the mathematical model, *i. e.* to converge. The convergence requirements for shape functions of an isoparametric element can be grouped into three categories, that is: completeness, compatibility and stability [1, 2].Consequently, we may say that consistency and stability imply convergence.

Completeness criterion requires that elements must have enough approximation power to capture the analytical solution in the limit of a mesh refinement process. Therefore, the finite element approximation functions must be of certain polynomial order ensuring that all integrals in the corresponding weak formulation have measurable values. Specifically, if m is variational index calculated as the highest spatial derivative order that appears in the energy functional of the relevant boundary value problem, than the element base approximation functions must represent exactly all polynomial terms in order m 1 in element coordinate system. A set of shape functions that satisfies this condition is called m-complete.

Further, compatibility criterion requires that finite element shape functions should provide temperature continuity between elements, in order to provide that no artificial temperature gaps will appear during heat transfer. As the mesh is refined, such gaps could multiply and may absorb or release spurious energy. So, patch trial functions must be C^{m-1} continuous between interconnected elements, and C^m piecewise differentiable inside each element.

Nevertheless, completeness and compatibility are two aspects of *so-called* consistency condition between mathematical and discrete models. Consequently, a finite element model that passes both completeness and continuity requirements is called consistent.

Further, if considered finite element is stable, non-physical zero-energy modes in finite element model problem will be prevented. The overall stability of mixed formulations is provided if two necessary conditions for stability are fulfilled *i. e.*, the first condition represented by the ellipticity on the kernel condition and second condition represented by the inf-sup condition [1, 2].

It should be noted that satisfaction of the completeness criterion is necessary for convergence of the finite element solutions, while violating other two criterions does not necessary mean that solution will not converge.

Consistency condition for finite element HC(8-20)/(9-27)

Presently, variational indices for temperature variable field and flux variable field are both $m = 1$. Further, in the present formulation, test and trial temperature and heat flux approximation functions are chosen to be from the sub-space $H^1(\Omega)$, as it can be seen from expression (11). Consequently, they are chosen to have C^0 continuity, *i. e.* they

are continuous, with finite first derivatives. Accordingly, the completeness and compatibility requirements for both fields are satisfied in the present case.

Nevertheless, it should be noted that from the reason that flux derivatives do not appear in the present formulation (10), the over-constrained continuity requirement on the heat flux's trial and test shape functions may be relaxed to be from sub-space L^2 *i. e.* discontinuous, between the finite elements if it is physically justified, as in the case of the abrupt material changes (on the interface of two materials).

First stability condition

The mixed formulation that we are considering can be written in the form

$$B[(T, q), (\theta, Q)] = F(\theta, Q) \tag{14}$$

where

$$B[(T, q),(\theta, Q)] \quad \int_\Omega qk^{-1} {:} Qd\Omega \quad \int_\Omega T \quad Qd\Omega \quad \int_\Omega q \quad \theta d\Omega \tag{15}$$

for $(T, q),(\theta, Q) \quad H^1(\Omega) \quad L_2(\Omega)^n$

i. e.

$$B[(T, Q),(\theta, q)] = a(q, Q) + b(T, Q) - b(\theta, q) \tag{16}$$

A major difficulty arises when we try to prove if the chosen finite element spaces yield stable approximations. The first stability condition stability can be proved if the bilinear form $B[(T, q), (\theta, Q)]$ is coercive.

Note that in this case, although B is not coercive, at least a is, *i. e.* the inequality $a(Q,Q) \quad \alpha\|Q\|^2$ for all $Q \quad L_2$ holds for some positive constant α.

However, the condition that the a form is coercive is not satisfied for most mixed methods. It turns out that one can get by with a weaker condition than coercivity of a on L_2, namely coercivity on a particular subspace H^1. More precisely, suppose that a positive constant α_h exists, such that

$$a(z,z) \quad \alpha_h\|z\|^2 \quad \text{for all} \quad z \quad Z_h, Z_h \quad \{z \quad \vartheta_h | b(v,z) \quad 0 \quad \text{for all} \quad v \quad \Theta_h\} \tag{17}$$

where ϑ_h and Θ_h are flux and temperature test approximation functions respectively. It should be noted that presently, test and trial flux local approximation functions are from continuous finite element subspace $\vartheta_h \quad (H^1)^n$. In fact, any choice of subspaces $\vartheta_h \quad (H^1)^n$ yields stable approximation [2], from the reason that the corresponding bilinear form is quadratic.

In addition, in the analysis of the present mixed formulation, a is positive definite, symmetric and bounded, and eq. (17) is satisfied for all $Q \quad _h$. Consequently, in the present problem a is coercive.

120

Hence, the first stability condition of the present finite element family is satisfied *a priori*.

Second stability condition

For the present finite element, the second stability condition is satisfied if value γ_h, following from LBB (Ladyzhenskaya, Babuška, Brezzi) condition (see [13], p. 76, eq. 3.22), remains bounded above zero for the meshes of increasing density:

$$\gamma \leq \gamma_h = \inf_{T \in H^1} \sup_{Q \in (H)^n} \frac{b(Q_h, T_h)}{\|Q_h\| \|T_h\|} \tag{18}$$

where

$$b(Q_h, T_h) = \sum_e \int_{\Omega_i} Q_h \cdot T_h d\Omega_e \tag{19}$$

$$\|Q_h\|^2 = \sum_e \int_{\Omega_i} Q_h \cdot Q_h d\Omega_e \tag{20}$$

$$\|T_h\|^2 = \sum_e \int_{\Omega_i} T_h \cdot T_h d\Omega_e \tag{21}$$

In addition, condition (18) ensures solvability and optimality of the finite element solution [11]. It should be emphasized also, that boundary conditions per temperature do not enter the present test.

Because verification of the condition like (18) involves an infinite number of meshes, it can not be performed analytically. Therefore, numerical inf-sup [1] test should be performed for a limited number of meshes of increasing refinement. Consequently, in the present case, numerical inf-sup test is represented by generalized eigenvalue problem, in matrix notation given by:

$$B_h A^{-1} B_h^T x = \lambda K_h x \tag{22}$$

where B and A are matrix entries in expression (12). Further, matrix K is the system matrix from the corresponding standard primal steady state heat finite element method, where entries are given by:

$$K_{LM} = \sum_e \int_{\Omega_e} P_{L,c} k^{cd} P_{M,d} d\Omega_e \tag{23}$$

The square root of the smallest eigenvalue of the problem (22), that is $(\lambda_{\min})^{1/2}$, is equal to the inf-sup value γ_h in condition (18). If the inf-sup values, for chosen sequence of finite element meshes, do not show decrease toward zero (meaning that $\lambda_{\min}$ values stabilize at some positive level) it can be said that the element passes the inf-sup test. It should be noted that decreasing of the inf-sup values on log-log diagram would be seen as

121

a curve with moderate or excessive slope. This approach was already used in [14] for testing the stability of quadrilateral finite elements QC4/5 and QC4/9, and in [5, 15] for testing the stability of the hexahedral finite element HC8/9 in linear elasticity. Nevertheless, the investigation whether the present finite elements passes numerical inf-sup test (22) is left for future report.

Numerical experiments

Although some exact solutions are available in standard references, there are few three-dimensional cases available. In the present section proposed method is tested on the several standard benchmark examples in steady state heat analysis. Size of elements is chosen to achieve reasonable engineering accuracy with reasonable computing times. Only those results for which the theoretical solution is known are given, while other results available from the analyses are not reported here.

Cooling of the still rod

A nickel-steel rod of length $l = 0.1$ and radius $r = 0.01$ [9] initially held at a uniform temperature of 200 °C is suddenly exposed to the environmental temperature $T_a = 30$ °C. One end of the nickel-steel rod is heated to the temperature of $T = 200$ °C. The other end is insulated, so there are no any boundary conditions per temperature or heat flux. The material thermal conductivity is 12 W/m°C, while the convective heat transfer coefficient is 22.11 W/m^2°C.

Present solutions are obtained using hexahedral meshes HC20/21 of increasing refinement along the rod longitudinal axe (z–axe), while refinement x-y in plane is shown in fig. 2. The relative absolute error, for the results obtained with several present finite element configuration, in accordance to 1-D are shown in fig. 3.
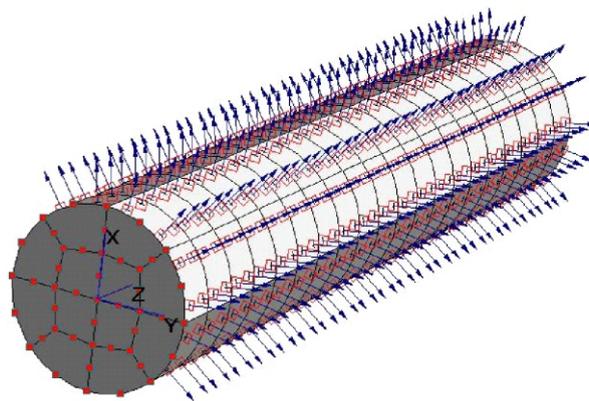

Figure 2. Cooling of the still rod model problem

From the fig. 3 we can see excellent agreement with theoretical results obtained by one-dimensional theory, which is less than 0.8% in error for all monitored rod's sections.
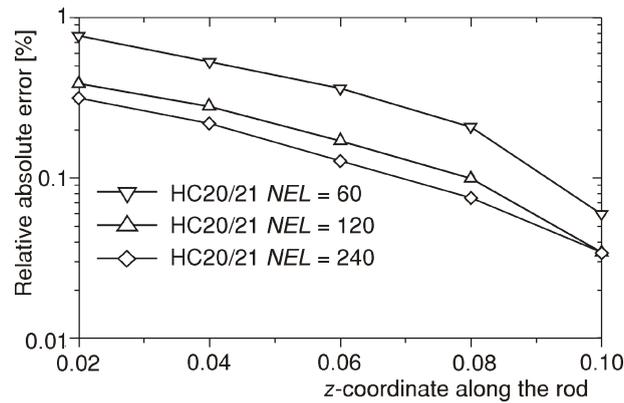

Figure 3. Solid billet: the relative absolute error in accordance to 1-D theory

Solid steel billet

In the present example steady state heat transfer in a solid steel billet [7], shown in fig. 4, is analyzed. Fixed temperatures are applied on the two end surfaces, and forced convention on the other faces. The target value is temperature at the point A, that is $T^A = 32.8$ °C. The material thermal conductivity is 50 W/m°C, while the heat transfer coefficient is 100 W/m²°C. Ambient bulk fluid temperature is 0 °C.

Figure 4. Solid steel billet model problem
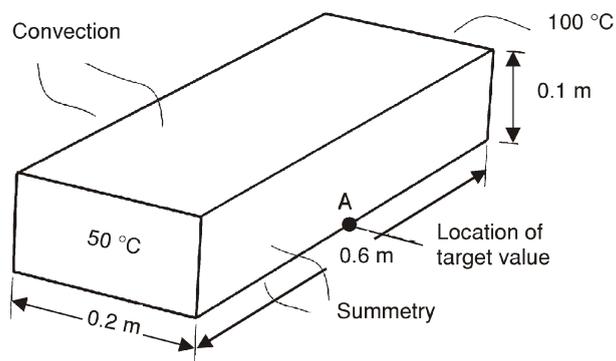
The model is discretized by increasing sequence of the refinement factors $N = 4$, 6, 8, 10, 12, and 14 and $L = 3, 4, 5, 6, 7$, and 8, where distribution of finite elements is given by the pattern $N \quad 3N \quad L$ along x, y and, z axes, respectively, in order to check the convergence of the finite element solutions.

From the temperature results at the target point with coordinates (0.2, 3, 0.0), we may see that both finite element approaches, present HC8/9 and primal HEXA8, converge uniformly to the same value which is less than 1% lower than target value (fig. 5).
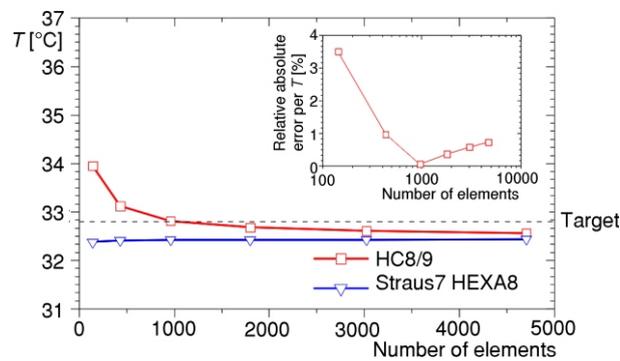
Figure 5. Solid billet: the convergence of temperature at target point

Nevertheless, the main difference is in calculation of heat flux field. In the primal approach (Straus7) it is calculated *a posteriori* that results with abnormal discontinuity along element interfaces (see fig. 6 on the left), which raise the need for the use of some recovery or smoothing technique of the heat flux (dual) variable [8]. On the other hand, presently heat flux field is calculated as the fundamental variable and it is continuous as it is expected to be (see fig. 6 on the right).
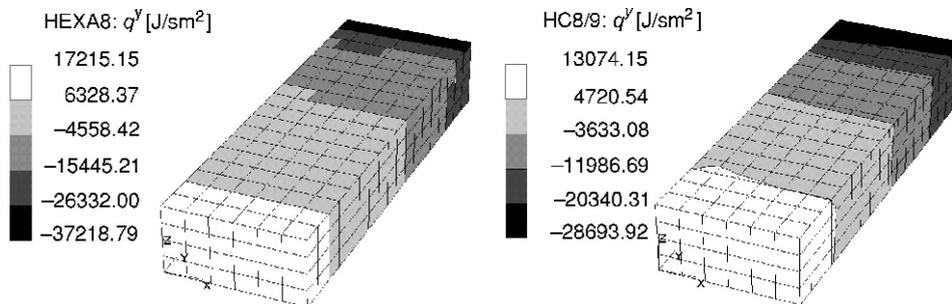

Figure 6. Heat flux q^y calculated by the primal (left) and present mixed approach (right)

Hollow cylinder with fixed temperature BC's

In this example heat transfer through a hollow cylinder is analyzed. Fixed temperature $T = 20$ °C is prescribed on the outer surface of the cylinder, and convection occurs on the inner surface. Fluid inside the cylinder is air, convection coefficient between inner wall of the cylinder and air is 30 W/m°C , and the air temperature is $T = 100$ °C.

Finite element model is three-dimensional section of the hollow cylinder with one layer of HC20/21 elements along the axis of the cylinder. Only one quarter of the model is analyzed due to the symmetry. Target value is the temperature on the inner surface [17]. The convergence of the results is shown in the fig. 7. In the same figure one can also see the size of the relative error compared to the exact theoretical solution.
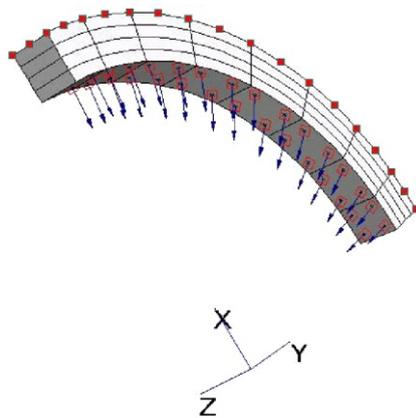

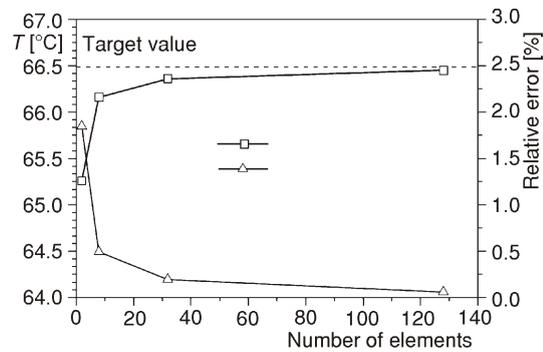**Figure 7. Hollow cylinder**

Figure 8. Hollow cylinder: Temperature result at target point and relative errors

From the results reported in fig. 8, we may notice that present finite element scheme instantly converge to the target result.

Hollow sphere with two materials and convective BC's

Steady state heat transfer through a sphere made of two materials is analyzed [18]. The inner radius is of 0.30 m, the interfacial radius is 0.35 m, and outer radius is 0.37 m. The sphere has convection boundary conditions, both on the inner and outer surface. On the outer surface, convection coefficient is 200 W/m²°C, and on the inner surface its value is 150 W/m²°C. Fluid inside and outside of the sphere is air. Its temperature inside the sphere is T = 70 °C and outside is T = –9 °C. Thermal conductivities of the materials are 40 W/m°C (inner sphere) and 20 W/m°C (outer sphere). In this example the inner (A), material boundary (B), and outer surface (C) temperatures are determined.

Only 1/8 of the sphere (as shown in fig. 9) has been analyzed, due to the symmetry. Finite element HC 20/21 has been used for this model, because it utilizes tri-quadratic approximation of geometry, temperature and heat flux. The four finite element meshes considered are shown in fig. 9.
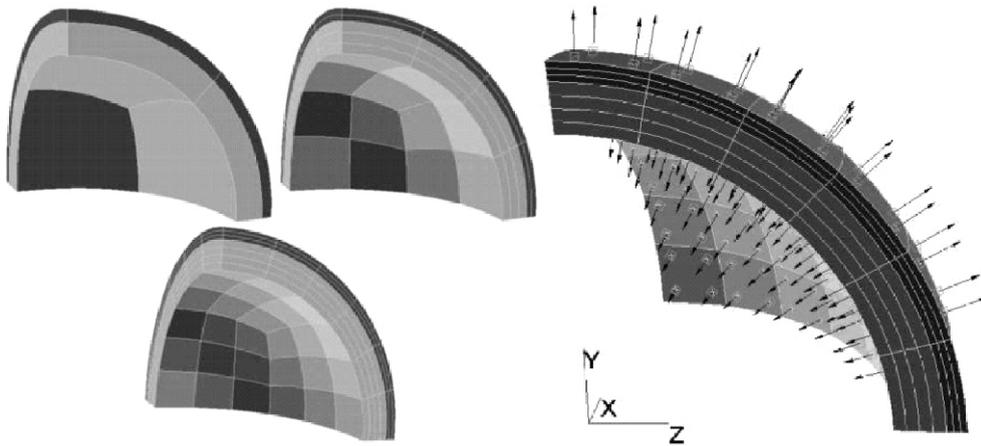

Figure 9. Two-material hollow sphere

Results for temperature values on three radii of the presently considered sphere namely at nodes A, B, and C, are shown in the tab. 3, as well as figs. 10 and 11.

Table 3. Temperature values on three radii of the sphere

NEL	T(A)	T(B)	T(C)
6	25.03	17.66	12.93
60	24.95	17.7	13.03
189	24.9	17.66	12.99
432	24.87	17.63	12.97
Target	25.06	17.84	13.16

From the results reported in the figs. 10 and 11, we may see that present solutions converges to some new target values that are a little bit lower in accordance to the given ones [18]. Nevertheless, for all considered target points relative error per finite element mesh in accordance to the target result, is less than 1.75%.
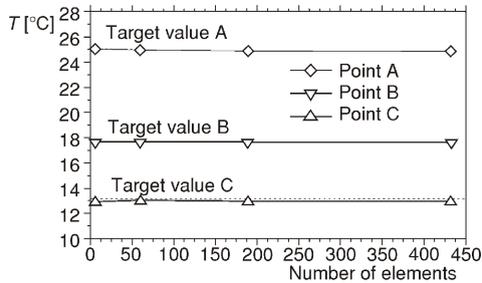
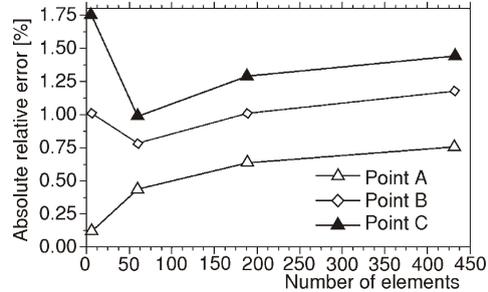**Figure 10. Convergence of the temperature values on three radii of the sphere**

Figure 11. Relative errors of calculated temperature values compared to the exact solutions

Conclusion

In the present text, mathematical aspect of convergence of the proposed finite element family HC(8-20)/(9-27), are analyzed. It is proven that present finite element family is consistent, solvable, and passes first stability condition. Further, from the standard benchmark examples in steady state heat analysis of solid bodies solved by the present finite element family, we may preliminary conclude that it converges regardless of the geometry, abrupt material changes, or distortion of the finite element (*e. g.* excessive thickness ratio). Moreover, we may emphasize that one of the main potentials of the present hexahedral finite element is in overcoming of well-known transition problem of connecting finite elements of different types and dimensions.

Consequently, we may end with conclusion that present finite element approach gives us greater design freedom than standard primal approaches that use different kind of finite elements: solid, plate/shell, beam. It should be noted that temperature results obtained by the present approach are a little bit lower than available target results. In addition, present finite element approach will be used in connection with the existing in-house software [5], based on the original reliable mixed displacement/stress finite element approach in elastic analysis, which is new original weakly coupled mixed steady state heat / thermoelasticity finite element approach in literature, with unique design characteristics.

Nomenclature

A	– surface area
A_{LpMr}	– members of the entry matix A which connect component p of the heat flux at nodal point L with component r of the heat flux at nodal poin M
$a\,(q,Q)$	– bilinear form
$B[(T, q), (\theta, Q)]$	– bilinear form

B_{LpM} – members of the entry matrix B which connect component p of the heat flux at nodal poin L with temperature at nodal point M

$b\,(T,\,\boldsymbol{Q})$– bilinear form

C_h – partitioning of the domain Ω into elements Ω_i

C^m – space of all functions with continuous partial derivatives of order m

D_{LM} – members of the entry matrix D which represent contribution from convective heat transfer

$F_M, H_M,$ – members of the entry matrices F, H, K which represent contribution from the heat

K_M – sources, prescribed hat flux and convective heat transfer, respectively

f – heat source, [W/m^{2}K]

$g_{(L)p}^{a}$ – Euclidian shifting operator

g^{ab} – components of the contravariant fundamental metric tensors with respect to natural coordinate system ξ^a

$g^{(L)mn}$ – components of the contravariant fundamental metric tensors with respect to $y^{(L)n}$ coordinate system

$H_{(\mathrm{div})}$ – space of all vector fields which are square integrable and have square integrable divergence

H^1 – space of all scalar fields which are square integrable and have square intergable gradients

$h,\,g$ – elements of $L_2\,(\Omega)$

h_c – convective coefficient, [W/m^{2}K]

h_r – radiative coefficient

$\boldsymbol{k}$ – second order tensor of thermal conductivity

L_2 – Hilbert space of all real measurable square integral functions

$N,\,L$ – mesh refinement factors

NEL – number of elements

n – number of freedom degrees

$\boldsymbol{n}$ – outward unit surface normal

n_T – number of freedom degrees per temperature

n_q – number of freedom degrees per flux

$P_L,\,V_L$ – local base functions

p – index denoting prescribed values of temperature and heat flux

$\boldsymbol{Q}$ – test function per heat flux

Q_h – space of heat flux trial functions

$\boldsymbol{q}$ – heat flux, [W/m^2]

q_c – prescribed heat flux due to the convection

q_h – prescribed heat flux

q_r – prescribed heat flux due to the radiation

T – temperature, [K]

T_a – temperature of the surrounding medium, [K]

T_h – space of temperature trial functions

$T^L,\,\boldsymbol{q}^L$ – value of temperature and heat flux at the node L

x – column vector

$y^{(L)r}\,(r,\,s,\,t = 1,\,2,\,3)$ – coordinate system at each global node L, per heat flux

$z^i\,(i,\,j,\,k,\,l = 1,\,2,\,3)$ – global Cartesian coordinate system

Greek letters

$\alpha,\,\alpha_h,\,\gamma$ – positive constants

128

δ_{ij} – Cronecker symbol
σ – Stefan-Boltzmann constant
Θ_h – space of temperature test functions
θ – test function per temperature
θ_L – value of temperature and heat flux test functions at the node L
ϑ_h – space of heat flux test functions
$\underline{\Omega}$ – inner part of $\overline{\Omega}$
$\overline{\Omega}$ – closed and bounded domain of the Euclidian space E^n ($n = 1, 2, 3$)
Ω_i – elements of C_h
Ω – boundary of Ω
Ω_c – part of the boundary per heat flux due to the convection
Ω_r – part of the boundary per heat flux due to the radiation
Ω_T – part of the boundary per temperature
Ω_q – part of the boundary per heat flux
$^a(a, b, c, d = 1, 2, 3)$ – local natural (convective) coordinate systems ($a, b, c, d = 1, 2, 3$)

Subscripts

L – free index *i. e.* unrepeated index which doesn't take part in summation
v – index denoting variable values of temperature and heat flux
vp – index denoting matrix entries which multiply prescribed values of temperature and heat flux
vv – index denoting matrix entries which multiply variable values of temperature and heat flux
p – index denoting prescribed values of temperature and heat flux

Acknowledgements

References

[1] Bathe, K. J., The Inf-Sup Condition and Its Evaluation for Mixed Finite Element Methods, *Computers & Structures* (2001), 79, pp. 243-252
[2] Arnold, D. N., Mixed Finite Element Methods for Elliptic Problems, *Comput. Meth. Appl. Mech. Eng.* (1990), 82, pp. 281-300
[3] Miranda, S., Ubertini, F., On the Consistency of Finite Element Models, *Comput. Meth. Appl. Mech. Eng.* (2001), 190, pp. 2411-2422
[4] Cannarozzi, A. A., Ubertini, F., A Mixed Variational Method for Linear Coupled Thermoelastic Analysis, *International Journal of Solids and Structures* (2001), 38, pp. 717-739
[5] Mijuca, D., On Hexahedral Finite Element HC8/27 in Elasticity, *Computational Mechanics, 33* (2004), 6, pp. 466-480
[6] Duff, I. S., Gould, N. I., Reid, J. K., Scott, J. A., Turner, K., Factorization of Sparse Symmetric Indefinite Matrices, *IMA J. Numer. Anal.* (1991), 11, pp. 181-204

[7]   ***, G+DComputing, Straus7, Finite Element Analysis System Software Package – Verification Manual, www.strand.aust.com, Australia

[8]   Hinton, E., Campbell, J. S., Local and Global Smoothing of Discontinuous Finite Element Functions Using a Least Squares Method, *Int. J. Num. Meths. Eng.,* (1974), 8, pp. 461-480

[9]   Holman, J. P., Heat Transfer, McGraw-Hill, New York, 1990

[10]   Zienkiewicz, O. C., Zhu, J. Z., Taylor, R. L., Nakazawa, S., The Patch Test for Mixed Formulations. *Int. J. Numer. Meth. Eng.,* (1986), 23, pp. 1873-1883

[11]   Olson, M. D., The Mixed Finite Element Method in Elasticity and Elastic Contact Problems, in: Hybrid and Mixed Finite Element Methods (Eds. S. N. Atluri, R. H. Gallagher, O. C. Zienkiewicz), John Wiley & Sons, 1983, pp. 19-49

[12]   Kasper, E. P., Taylor, R. L., A Mixed-Enhanced Strain Method, Linear Problems. University of California, 1997, Report No.UCB/SEMM-97/02

[13]   Brezzi, F., Fortin, M., Mixed and Hybrid Finite Element Methods, Springer-Verlag, New York, 1991

[14]   Berković, M., Mijuca, D., On the Main Properties of the Primal-Mixed Finite Element Formulation, *Facta Universitatis Series Mechanics, Automatic Control and Robotics., 2* (1999), 9, pp. 903-920

[15]   Mijuca, D., A New Reliable 3D Finite Element in Elasticity, *Proceedings*, 5th World Congress on Computational Mechanics (WCCM V) (Eds. H. A. Mang, F. G. Rammerstorfer, J. Eberhardsteiner), Vienna University of Technology, Austria, 2002

[16]   Jarić, J., Continuum Mechanics (in Serbian), Gradjevinska knjiga, Belgrade, 1988

[17]   ***, French Society of Mechanics, Validation Commission for Software Packages for Numerical Calculation of Structures, Working Group for Heat Transfer (2D and 3D) and Thermoelasticity, TPLA 01/89, Paris, 1989

[18]   ***, French Society of Mechanics, Validation Commission for Software Packages for Numerical Calculation of Structures, Working Group for Heat Transfer (2D and 3D) and Thermoelasticity, TPLV 04/89, Paris, 1989

Authors' addresses:

D. M. Mijuca, A. M. Žiberna, B. I., Medjo
Faculty of Mathematics, University of Belgrade,
 11001 Belgrade, P. O. Box 550
Serbia and Montenegro